PROCEEDINGS OF SPIE

SPIEDigitalLibrary.org/conference-proceedings-of-spie

Widely-tunable single fiber laser OPO for multimodal microscopy

Cromey, Benjamin, Batjargal, Orkhongua, Qin, Yukun, Crystal, Sean, Kieu, Khanh

Benjamin Cromey, Orkhongua Batjargal, Yukun Qin, Sean Crystal, Khanh Kieu, "Widely-tunable single fiber laser OPO for multimodal microscopy," Proc. SPIE 11264, Nonlinear Frequency Generation and Conversion: Materials and Devices XIX, 112640C (2 March 2020); doi: 10.1117/12.2546599

SPIE.

Event: SPIE LASE, 2020, San Francisco, California, United States

Widely-tunable single fiber laser OPO for multimodal microscopy

Benjamin Cromey[1], Orkhongua Batjargal[1], Yukun Qin[1], Sean Crystal[1], and Khanh Kieu[1]

[1]James C. Wyant College of Optical Sciences, The University of Arizona, Tucson, 85721, USA

ABSTRACT

Raman microscopy is a key technique for biological imaging since it can provide valuable information about the chemical constituents of a sample without any labels. However, because two wavelengths are required for either CARS or SRS to occur, most Raman imaging set ups use multiple lasers with complicated synchronization requirements. In this presentation, we discuss the design and performance of a tunable Ytterbium-based fiber laser and an optical parametric oscillator for Raman microscopy. Our system uses a single laser that creates both pump and probe beams via nonlinear optical effects. Due to its reasonable high peak power, this laser system is a suitable light source for multimodal microscopy using both Raman and multiphoton imaging functionalities.

Keywords: Fiber laser, OPO, Stimulated Raman Scattering, multimodal microscopy, multiphoton microscopy

1. INTRODUCTION

Raman microscopy is a popular and effective nonlinear imaging technique that can be applied to many disciplines due to its ability to identify the chemical constituents of an object under test without labels.[1,2] The two common forms of Raman microscopy, stimulated Raman scattering (SRS) and coherent anti-Stokes Raman Scattering (CARS), can be combined with multiphoton imaging modalities such as two photon fluorescence and second harmonic generation for multimodal imaging.[3,4] Because multiphoton microscopy (MPM) can be another label-free technique, combining these different approaches is a strong potential path forward to faster and more accurate medical diagnoses since both MPM and Raman microscopy have demonstrated capabilities for identifying several diseases.[5–9] One of the drawbacks of most Raman imaging systems is their complexity. As a pump-probe imaging technique, both CARS and SRS require that two different laser wavelengths illuminate the sample in a synchronized manner. Additionally, these wavelengths need to be able to be tuned relative to each other, so that their combination is resonant with different vibrational transitions in the material. Synchronizing the pulse trains from two different laser systems requires complex electronics and co-alignment of the beams to be used in the microscope system. Most Raman imaging set-ups depend on bulky solid states lasers to provide a tunable, high peak power laser.[3,5,10–12] These lasers do give a widely tunable range, at the cost of a large, expensive laser with precise alignment requirements.

Several groups have attempted to address this concern through the use of fiber lasers, promising sources that can replace the Ti:Sa in several different areas of biological imaging.[3,10,11,13–17] Fiber lasers are ideal due to their lack of alignment needs and their compact form factor. Many of these are frequently paired with a second laser, since they only provide either the pump or the probe wavelength.[3,10,11] Ti:Sa lasers and ytterbium fiber lasers pair together very well for Raman, since the wavenumber difference between the light near 800 nm from the Ti:Sa and light near 1040 nm from the ytterbium falls within the CH region. An even more ideal configuration is using one fiber laser to produce both pump and probe wavelengths, either by frequency doubling the fundamental wavelength,[13,18] or through the use of an optical parametric oscillator.[14–17,19–21] These single laser solutions drastically simplify the synchronization needs. However, many of these systems are still limited by low tunability, such that they may cover the CH region, but not the any of the fingerprint region or silent region. Several of the cited works also incorporate free-space components, removing the alignment free benefit of a monolithic fiber system.[15,16] Fiber lasers have also had a great impact in the multiphoton microscopy realm, enabling a smaller form factor and alignment-free, reliable, high peak power sources[22]

Send correspondence to bcromey@email.arizona.edu

Nonlinear Frequency Generation and Conversion: Materials and Devices XIX, edited by Peter G. Schunemann, Kenneth L. Schepler, Proc. of SPIE Vol. 11264, 112640C
 · doi: 10.1117/12.2546599

In this work, we greatly simplify the optical system by creating both the pump and the probe beam from a single tunable picosecond Yb fiber laser and an all fiber optical parametric oscillator (OPO) based on LMA-PM5 photonic crystal fiber (PCF). By tuning both the oscillator central wavelength and the delay between the oscillator and the OPO, we can achieve a broad tunability. Paired with a new microscope design inspired by our previously demonstrated all reflective multiphoton microscope design, we will have a very simple and compact Raman imaging system.[23] This laser is an ideal source for multimodal microscopy. This presentation will cover the design and characterization of the laser source, as well as discuss its performance as a source for multimodal imaging.

2. LASER DESCRIPTION

The laser system is divided up into four main sections: a mode-locked picosecond Ytterbium oscillator, a pre-amplifier, a secondary Ytterbium amplifier, and finally a Fiber Optical Parametric Oscillator (FOPO) for generation of the pump or probe wavelength. Fig. 1 shows the schematic diagram of the full system, identifying the four segments that will be discussed in detail. The entire system uses polarization maintaining (PM) fiber.

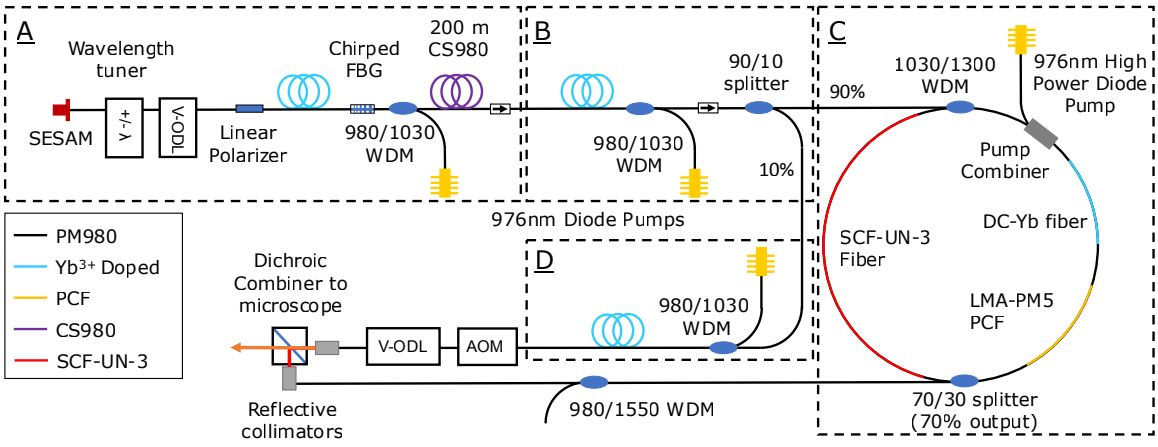

Figure 1. This laser system is divided into four sections, A: Oscillator, B: Pre-amplifier, C: FOPO, and D: Secondary amplifier. SESAM: Semiconductor saturable absorber Mirror. V-ODL: Variable optical delay line. WDM: Wavelength division multiplexer. FBG: Fiber Bragg Grating. DC: Double clad. AOM: Acousto-optic modulator. PCF: Photonic crystal fiber

The system begins with a conventional picosecond Ytterbium oscillator based on a semiconductor saturable absorber mirror (SESAM). As shown in the schematic diagram, Fig 1A, the oscillator consists of a SESAM, 50 cm of PM Yb-doped gain fiber, a linear polarizer to block lasing in the fast axis, a fiber-coupled delay line, a fiber-coupled tunable filter (1 nm bandwidth and tunable from 1010 nm to 1090 nm), and ends with a chirped fiber Bragg grating (CFBG) with 50% transmission and reflection throughout the tuning range. The 976 nm pump laser is coupled to the cavity from outside through the WDM. The oscillator provides a tunable output from 1025 to 1045 nm with a FWHM of 0.2 nm at a 43 MHz repetition rate, an output power of 3 mW, and a pulse duration of 5 ps. The oscillator is self-starting within the tunable regime. In order to reduce nonlinear distortion and spectral broadening to the 1 μm pulses in the next sections, 200m of CS980 fiber is used to up-chirp the pulses to 15 ps duration.

After this, a pre-amplifier (seen in Fig. 1B) brings the output power to 55 mW. This output is then split by 90% and 10% to seed the power amplifier inside the FOPO, and the secondary amplifier. The Ytterbium power amplifier for the FOPO is placed inside the FOPO cavity to reduce the nonlinear distortion to the 1 μm pump

pulses before the parametric gain fiber. The FOPO cavity is a ring cavity that consists of a 1030/1300nm filter based broadband PM WDM to insure idler resonant operation, a pump-signal combiner, PM 10/125 double-clad Ytterbium fiber, 20cm of LMA-PM5-PCF (NKT Photonics) as the parametric gain medium, a 70/30 output coupler (70% output, 30% feedback) and PM SCF-UN-3 fiber to provide normal dispersion to the cavity. The PCF is directly spliced to the other fibers, preserving the all-fiber format. For the Raman imaging application, a narrow spectral bandwidth is desirable to achieve high spectral resolution. For this reason, both the pump and idler were chirped with normal dispersion fiber. In this chirping arrangement, the OPO cavity will provide more narrow bandwidth, but will have less efficiency, since it will only phase match with a portion of the pump pulse. The synchronization between the FOPO and the 1 μm pump is achieved by the delay line inside the 1 μm pump oscillator.

In Fig. 1D, the secondary amplifier brings the small amount of power sent from the pre-amp up to a max of 300mW. After this, the laser output is collimated, sent through a free-space AOM, and then focused back into fiber for final delivery inside the microscope. A free space AOM was used out of availability, as it contributes much of the loss (≈70%) in this arm since the light has loss both from the efficiency of the AOM, and from the loss re-coupling into fiber.

3. LASER PERFORMANCE AND CHARACTERIZATION

The laser was characterized at each stage of construction. The output of the oscillator is shown below in Fig. 2, demonstrating a tunable range of slightly more than 20 nm. Next to it, the calculated phase matching curve for the PCF fiber is shown, based on well-characterized parameters of the fiber in the literature.[24,25] With the pump light tunable from 1025nm to 1046nm, and the idler tunable from 1534nm to 1275nm, we expected that the laser should reach Raman resonances from 3237cm^{-1} to 1717cm^{-1}, or a range of 1520cm^{-1}. This would cover all of the CH region, the silent region, and the top end of the fingerprint region. We chose to work with the idler instead of the signal wavelength since longer wavelengths have been shown to have better penetration depth.[26]

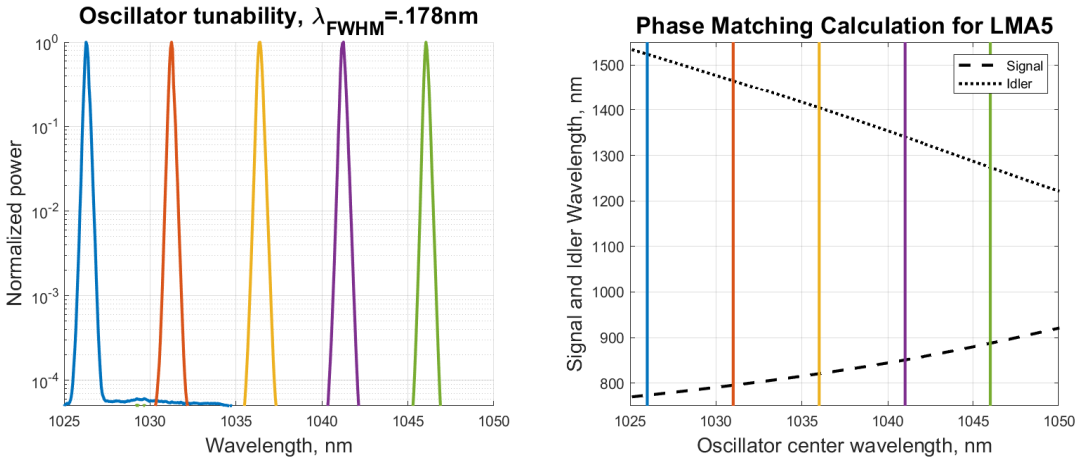

Figure 2. Left, tunable oscillator output spectra. Right, the phase matching curves for the PCF are plotted for both the signal and the idler. The center wavelengths shown on the left are also plotted in the same color to indicate which wavelengths would be phase-matched in the OPO along the phase matching curves.

Output spectra from all sections of construction are shown in Fig. 3. For each graph, the data is shown at 1029nm, since this was calculated to provide a Raman resonance near 2950cm^{-1}, a key CH resonance.

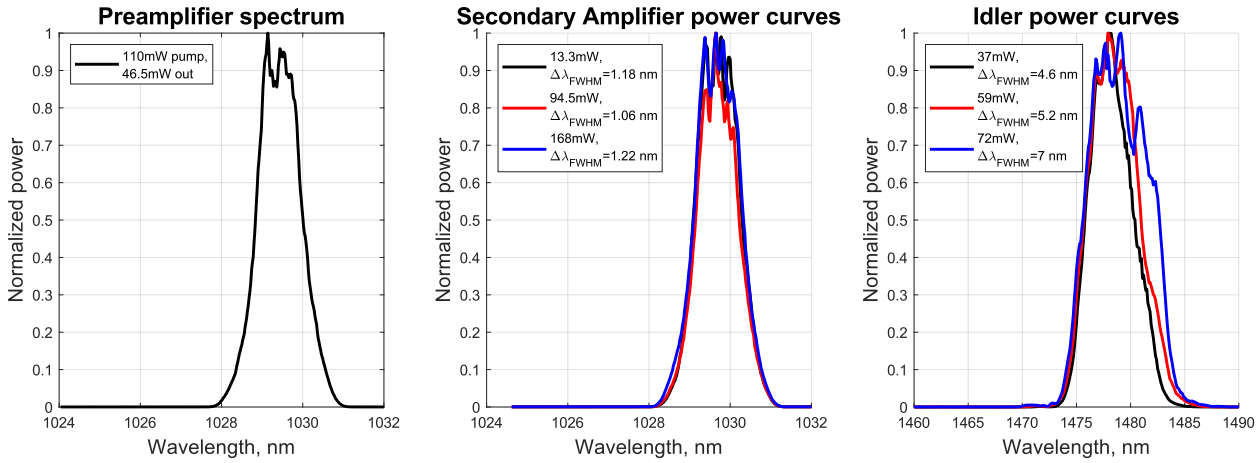

Figure 3. The performance of the laser at several points operating near a key CH bond resonance. The preamplifier spectrum is shown, which does not have its power adjusted for each configuration. The main amplifier power is shown at various pump powers, with clear peaks formed as a result of SPM. The secondary amplifier maintains a small bandwidth of 1 nm, which is important for higher spectral resolution. The idler performance is also shown.

The secondary amplifier maintains a narrow bandwidth of 1.28 nm, giving it a spectral resolution of $12cm^{-1}$. The idler output has less spectral resolution, with an average bandwidth of 7.3 nm. The pulse widths of the secondary amplifier output and the OPO output were 15 ps and 5 ps, respectively.

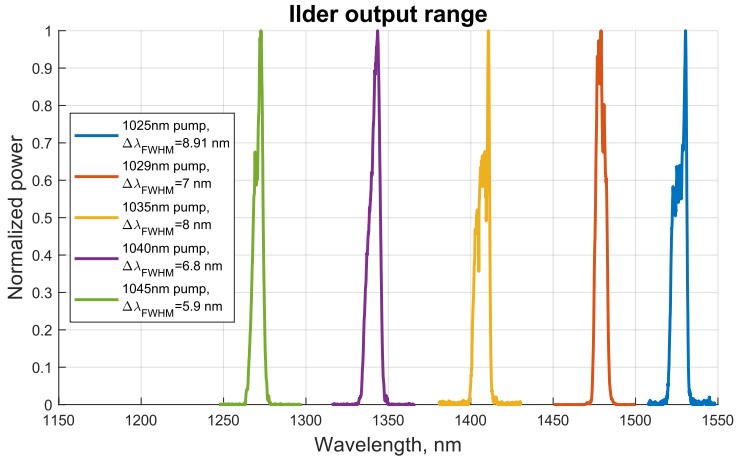

Figure 4. The normalized ilder output at several different pump wavelengths and pump powers are plotted in linear scale, accompanied by their spectral FWHM and output power. Each plot has a window of 30 nm for a fair comparison of bandwidths

The demonstrated tuning range is from 1707-3220cm^{-1}, which is 1513cm^{-1}.

4. IMAGES CAPTURED USING THE LASER

The laser was coupled into a new all-reflective system and used to image various samples. An 1150nm long pass dichroic mirror was used to combine the two beams to send into the microscope optical system. To maintain the all-reflective nature, a 15x .58NA reflective microscope objective from Spectra-Tech Inc. was used. Images from three different samples are presented, captured using two different multiphoton imaging processes, two photon excitation fluorescence (2PEF), and third harmonic generation (THG).

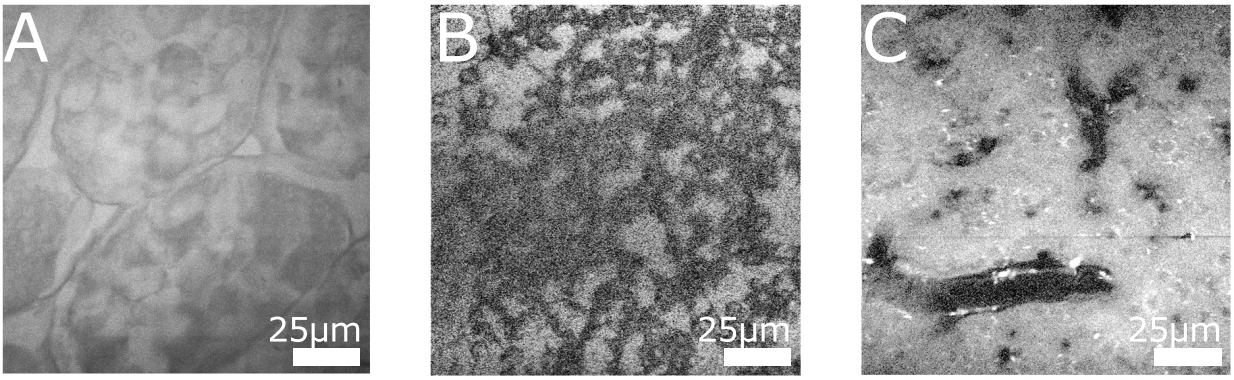

Figure 5. Multiphoton images of three different samples. A: 2PEF image of a pisum seed sample. B: THG image of high-fatty mouse liver tissue. C: THG image of a mouse brain section.

5. CONCLUSIONS AND FUTURE PLANS

A single fiber laser that can produce both the pump and the probe beam for Stimulated Raman Scattering was proposed, designed, and assembled. The laser was characterized in its tunability and spectral FWHM at multiple idler wavelengths. Future work on this project includes more imaging using the new all reflective system to further demonstrate the utility of a tunable source inside a system with no chromatic effects. Further optimization will be performed to streamline the laser system and increase the efficiency of the OPO, as well as switching to a fiber-coupled AOM to increase the pump power.

ACKNOWLEDGMENTS

Funding for this project was provided by The National Science Foundation (NSF) through a Graduate Research Fellowship (DGE-1143953) and NSF ECCS (1610048), the ARCS Foundation, and The National Institutes of Health (NIH) (1R01EB020605).

The liver tissue sample was provided by Dr. Timothy Lee at the University of Nevada Las Vegas. The mouse brain tissue was provided by Dr. Arthur Rigel at the University of Arizona.

REFERENCES

[1] Freudiger, C. W., Min, W., Saar, B. G., Lu, S., Holtom, G. R., He, C., Tsai, J. C., Kang, J. X., and Xie, X. S., "Label-free biomedical imaging with high sensitivity by stimulated raman scattering microscopy," *Science* **322**(5909), 1857–1861 (2008).

[2] Evans, C. L. and Xie, X. S., "Coherent anti-stokes raman scattering microscopy: Chemical imaging for biology and medicine," *Annual Review of Analytical Chemistry* **1**(1), 883–909 (2008).

[3] Meyer, T., Chemnitz, M., Baumgartl, M., Gottschall, T., Pascher, T., Matthäus, C., Romeike, B. F. M., Brehm, B. R., Limpert, J., Tünnermann, A., Schmitt, M., Dietzek, B., and Popp, J., "Expanding multimodal microscopy by high spectral resolution coherent anti-stokes raman scattering imaging for clinical disease diagnostics," *Analytical Chemistry* **85**(14), 6703–6715 (2013).

[4] Wang, Z., Zheng, W., Hsu, C.-Y. S., and Huang, Z., "Polarization-resolved hyperspectral stimulated raman scattering microscopy for label-free biomolecular imaging of the tooth," *Applied Physics Letters* **108**(3), 033701 (2016).

[5] Antonio, K. A. and Schultz, Z. D., "Advances in biomedical raman microscopy," *Analytical Chemistry* **86**(1), 30–46.

[6] You, S., Sun, Y., Chaney, E. J., Zhao, Y., Chen, J., Boppart, S. A., and Tu, H., "Slide-free virtual histochemistry (part i): development via nonlinear optics," *Biomedical Optics Express* **9**(11), 5240 (2018).

[7] You, S., Sun, Y., Chaney, E. J., Zhao, Y., Chen, J., Boppart, S. A., and Tu, H., "Slide-free virtual histochemistry (part II): detection of field cancerization," *Biomedical Optics Express* **9**(11), 5253 (2018).

[8] Hoover, E. E. and Squier, J. A., "Advances in multiphoton microscopy technology," **7**(2), 93–101 (2013).
[9] Zipfel, W. R., Williams, R. M., and Webb, W. W., "Nonlinear magic: multiphoton microscopy in the biosciences," *Nature Biotechnology* **21**(11), 1369–1377 (2003).
[10] Ozeki, Y., Asai, T., Shou, J., and Yoshimi, H., "Multicolor stimulated raman scattering microscopy with fast wavelength-tunable yb fiber laser," *IEEE Journal of Selected Topics in Quantum Electronics* **25**(1), 1–11.
[11] Ozeki, Y., Umemura, W., Otsuka, Y., Satoh, S., Hashimoto, H., Sumimura, K., Nishizawa, N., Fukui, K., and Itoh, K., "High-speed molecular spectral imaging of tissue with stimulated raman scattering," *Nature Photonics* **6**(12), 845–851.
[12] Ito, T., Obara, Y., and Misawa, K., "Invited article: Spectral focusing with asymmetric pulses for high-contrast pump–probe stimulated raman scattering microscopy," *APL Photonics* **3**(9), 092405 (2018).
[13] Freudiger, C. W., Yang, W., Holtom, G. R., Peyghambarian, N., Xie, X. S., and Kieu, K. Q., "Stimulated raman scattering microscopy with a robust fibre laser source," *Nature Photonics* **8**(2), 153–159.
[14] Kieu, K., Saar, B. G., Holtom, G. R., Xie, X. S., and Wise, F. W., "High-power picosecond fiber source for coherent raman microscopy," *Optics Letters* **34**(13), 2051.
[15] Lamb, E. S., Lefrancois, S., Ji, M., Wadsworth, W. J., Sunney Xie, X., and Wise, F. W., "Fiber optical parametric oscillator for coherent anti-stokes raman scattering microscopy," *Optics Letters* **38**(20), 4154 (2013).
[16] Gottschall, T., Meyer, T., Baumgartl, M., Dietzek, B., Popp, J., Limpert, J., and Tünnermann, A., "Fiber-based optical parametric oscillator for high resolution coherent anti-stokes raman scattering (CARS) microscopy," *Optics Express* **22**(18), 21921 (2014).
[17] Baumgartl, M., Gottschall, T., Abreu-Afonso, J., Díez, A., Meyer, T., Dietzek, B., Rothhardt, M., Popp, J., Limpert, J., and Tünnermann, A., "Alignment-free, all-spliced fiber laser source for CARS microscopy based on four-wave-mixing," *Optics Express* **20**(19), 21010 (2012).
[18] Gambetta, A., Kumar, V., Grancini, G., Polli, D., Ramponi, R., Cerullo, G., and Marangoni, M., "Fiber-format stimulated-raman-scattering microscopy from a single laser oscillator," *Optics Letters* **35**(2), 226.
[19] Hanninen, A. M., Prince, R. C., and Potma, E. O., "Triple modal coherent nonlinear imaging with vibrational contrast," *IEEE Journal of Selected Topics in Quantum Electronics* **25**(1), 1–11.
[20] Brinkmann, M., Janfrüchte, S., Hellwig, T., Dobner, S., and Fallnich, C., "Electronically and rapidly tunable fiber-integrable optical parametric oscillator for nonlinear microscopy," *Optics Letters* **41**(10), 2193 (2016).
[21] Brinkmann, M., Brinkmann, M., Brinkmann, M., Fast, A., Fast, A., Hellwig, T., Hellwig, T., Pence, I., Evans, C. L., Fallnich, C., and Fallnich, C., "Portable all-fiber dual-output widely tunable light source for coherent raman imaging," *Biomedical Optics Express* **10**(9), 4437–4449 (2019).
[22] Kieu, K., Mehravar, S., Gowda, R., Norwood, R. A., and Peyghambarian, N., "Label-free multi-photon imaging using a compact femtosecond fiber laser mode-locked by carbon nanotube saturable absorber," *Biomed. Opt. Express* **4**, 2187–2195 (Oct 2013).
[23] Amirsolaimani, B., Cromey, B., Peyghambarian, N., and Kieu, K., "All-reflective multiphoton microscope," *Optics Express* **25**(19), 23399–23407.
[24] Zlobina, E. A., Kablukov, S. I., and Babin, S. A., "Tunable CW all-fiber optical parametric oscillator operating below 1 m," *Optics Express* **21**(6), 6777–6782 (2013).
[25] Zlobina, E. A., Kablukov, S. I., and Babin, S. A., "Phase matching for parametric generation in polarization maintaining photonic crystal fiber pumped by tunable yb-doped fiber laser," *JOSA B* **29**(8), 1959–1967 (2012).
[26] Moester, M. J. B., Zada, L., Fokker, B., Ariese, F., and Boer, J. F. d., "Stimulated raman scattering microscopy with long wavelengths for improved imaging depth," *Journal of Raman Spectroscopy* **50**(9), 1321–1328 (2019).